Flash-flood hydrology and aquifer-recharge in Wadi Umm Sidr, Eastern Desert, Egypt

Mahmoud Abbas[a,b], Paul A. Carling[d *], John D. Jansen[e], Bety S. Al-Saqarat[f]

[a] School of Earth Sciences, China University of Geosciences, 430074, Wuhan, China.
[b] Luminescence Dating Laboratory, Three Gorges Research Center for Geo-hazards, China University of Geosciences, Wuhan 430074, China. Subariny_m2008@yahoo.com
[d] Geography and Environment, University of Southampton, Highfield, Southampton, SO17 1BJ, UK. P.A.Carling@soton.ac.uk, ORCID 0000-0002-8976-6429
[e] GFÚ Institute of Geophysics, Czech Academy of Sciences, 141 31 Prague, Czechia. jdj@ig.cas.cz, ORCID 0000-0002-0669-5101
[f] Department of Geology, The University of Jordan, Amman 11962, Jordan. b.saqarat@ju.edu.jo, ORCID 0000-0002-6933-0150

*Corresponding author

Abstract

Rapid urbanization and irrigation agriculture along the hyperarid Red Sea coastal plain in Egypt are dependent on freshwater supply from coastal aquifers. The aquifers are recharged by flash-floods from catchments (wadis) in the Eastern Desert, but large floods also cause infrastructure damage and deaths. Flood management strategies require knowledge of flood magnitude-frequency relationships, but in this regard quantitative data are lacking. Here, we reconstruct the peak discharge of a large flash-flood in 2016 using field measurements and flood discharge modelling along Wadi Umm Sidr, ~ 50 km west of Hurghada. In addition, we estimated the total flood volume, the flood duration, the infiltration rate and the transmission losses. Results are consistent with the few published determinations for large floods across the wider Levant. Field survey of recent floods (and palaeofloods) is a robust means to develop regionally applicable magnitude-frequency relationships. We close with some recommendations regarding flood protection of the Red Sea coastal infrastructure.

Keywords: flash-floods, wadis hydrology, infiltration, transmission losses, aquifer-recharge, Eastern Desert, Egypt.

Graphical Abstract

Flash-flood hydrology and aquifer-recharge in Wadi Umm Sidr, Eastern Desert, Egypt

Mahmoud Abbas, Paul A. Carling [*], John D. Jansen, Bety S. Al-Saqarat

[*]Corresponding author

Modelling of field evidence provides estimates of the 2016 regional flood for a major stream course, draining to the Red Sea coast of Egypt, yield peak flow of $500 m^3 s^{-1}$ equivalent to unit-area discharges of 4.85 to 8 $m^3 s^{-1} km^{-2}$, which lie below but close to regional flood envelop curves. The transmission losses between the range front and the coast are ~ 30 % of the upstream flood volume, consistent with transmission losses elsewhere in the region.

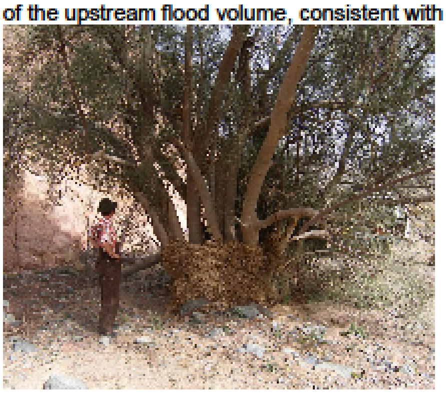

Vegetation debris 1.5m high represents level of 2016 flood in hyperarid Wadi Umm Sidr, Egypt.

1. Introduction

The National Economy plan for Egypt includes a focus on development of the hyperarid Eastern Desert (Fig. 1). Development, including tourism, industry and irrigation agriculture, requires adequate water resources, increasingly met from groundwater pumped at shallow depths from the Lower Miocene Ranga aquifer (Abdalla *et al*., 2014; Abdalla, Mekhemer, Abdallah Mabrou, 2016). And yet, little is known of the recharge potential of this sandy-gravel body from surface runoff (Moneim, 2005). Surface water flow occurs when the aquifer is fully saturated (Geith & Sultan, 2002) or, more usually, when the delivery of flood water to the ground-surface is in excess of the infiltration rate. In either case, the presence of surface water flow equates to alluvial aquifer recharge frequency. Groundwater extraction projects for irrigation in the Eastern Desert frequently involve creation of surface-water detention basins on the coastal plain that are subject to substantial infiltration and evaporative losses. These detention basins have potential to refill during flash floods and there is the risk of breaching the sandy bunds, which might exacerbate flooding of major coastal communities, such as Hurghada (Abd-Elhamid, Ismail Fathy, Zeleňáková, 2018). Sediment loads, scoured from the upper wadi beds by flash-floods contribute to the aggradation of the modern coastal plain, impact infrastructure and, on reaching the Red Sea, affect the marine environment. In this respect, there is a need for better understanding of the magnitude and frequency of wadi runoff events, infiltration and transmission losses. Here, we estimate the magnitude of a recent large flood and determine what transmission losses occurred downstream. The intention is to provide field data to aid planning decisions related to the management of floods from the Red Sea Mountains that drain to the rapidly urbanizing western shore of the Red Sea.

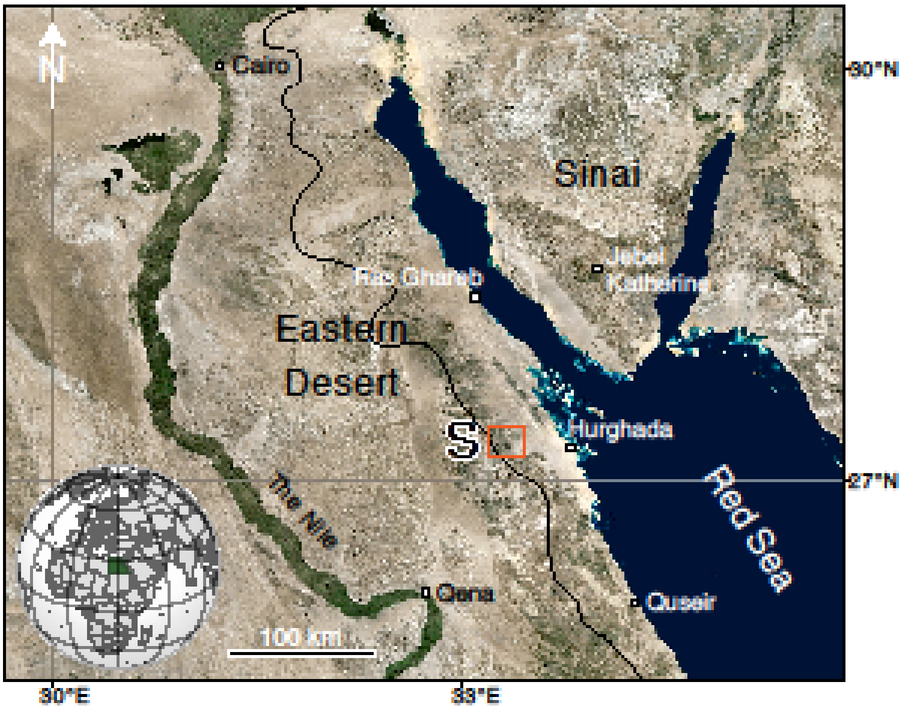

Figure 1: Location of the Wadi Umm Sidr study area (S) ~ 50 km west of Hurghada, and localities mentioned in the main text. Inset shows Egypt's global setting.

Moneim (2005) judged that the catchments to the west of Hurghada have relatively low groundwater recharge potential but high flash-flood risk. Abdel-Lattif & Sherief (2012) and Abdalla et al. (2014) made a general assessment of flash-flood risk in the Eastern Desert using an uncalibrated, distributed hydrological model (El-Shamy, 1992) but there are few such assessments (Mohamed, 2019). So, to address the lack of hydrological data from Eastern Desert wadis, we selected a drainage basin inland of Hurghada, Wadi Umm Sidr, for detailed investigation of recent flood history (Fig. 2). Wadi Sidr Is typical of larger catchments that occasionally produce floods that reach urbanized areas along the coast. The landscape setting is characterized below, after a consideration of the regional hydrology.

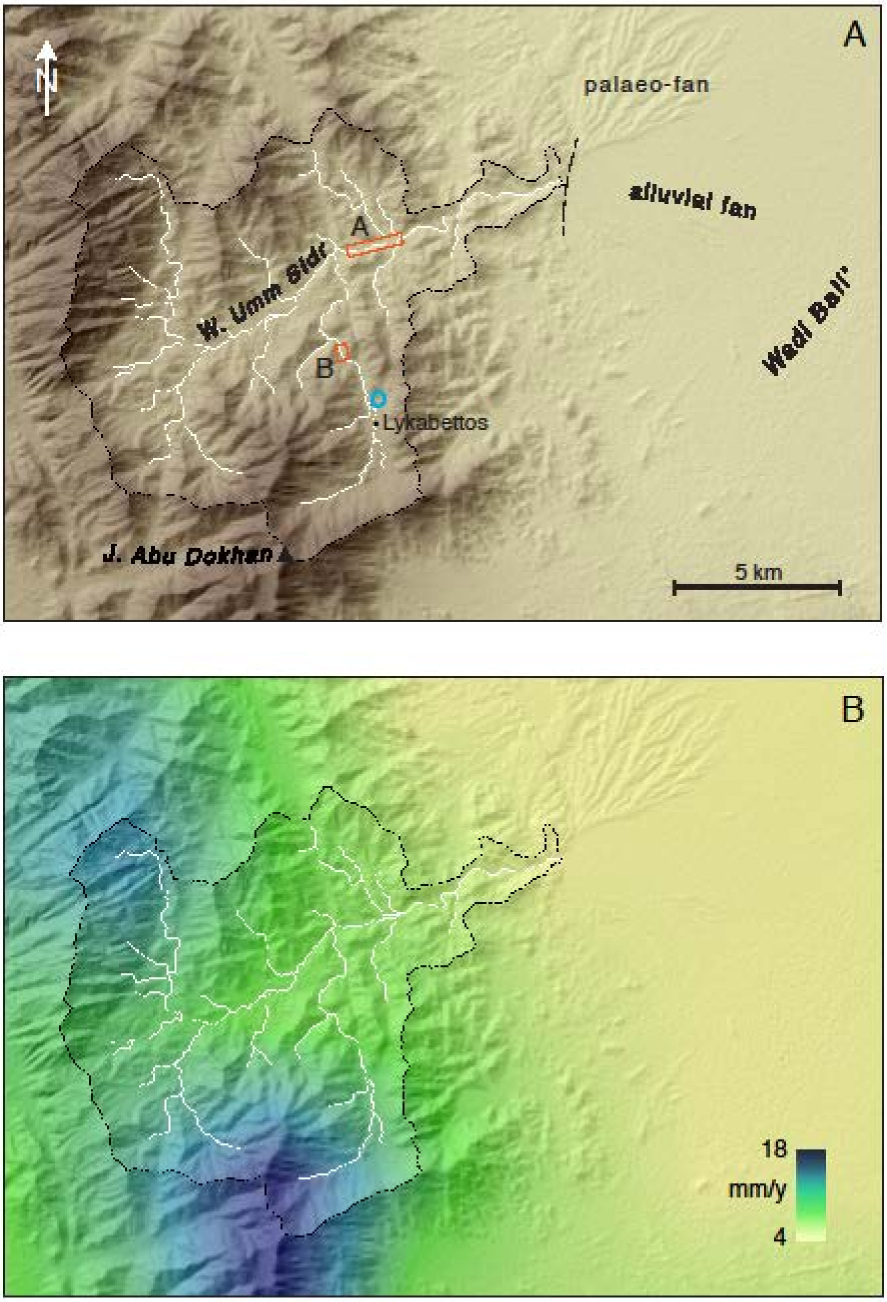

Figure 2: A) Wadi Umm Sidr catchment and highest peak, Jebel Abu Dokhan (1662 m). The catchment drains 103 km^2 of mountainous terrain with up to ~ 1300 m relief and debouches to an alluvial fan that feeds into the vast braiding channel system of Wadi Bali'*. Our flood discharge sites are shown in the wadi mainstem (box A) and in the right-bank tributary, Wadi Abu Ma'amel (box B), which drains 12.5 km^2. A Roman way station is also within box A, note the water well in a minor tributary (cyan circle) associated with the Roman village ruin, Lykabettos. Base map from Shuttle Radar Topographic Mission 1 arc-sec digital elevation*

*model. B**)** Estimated mean annual rainfall according to the WorldClim 2.0 dataset (Fick & Hijmans, 2017) for Wadi Umm Sidr, which applies spatial interpolation from Nile valley and coastal data for the period 1970–2000. Map shows a bilinear interpolation of 2.5′ resolution data; mean annual rainfall for the catchment is 10 mm yr^{-1}.*

2. Eastern Desert Regional Hydrology

The wadis of the Eastern Desert are ungauged and so little is known of the flood hydrology of the region, with meteorological data being available only from coastal stations and from Qena on the Nile (Moneim, 2005; Elsadek, Ibrahim, Mahmod, 2018). The region is hyperarid with Hurghada receiving an average annual rainfall of 3 mm, Quseir to the south, 4 mm, and Qena, 7 mm (Moeyersons, Vermeersch, Beeckman, Van Peer, 1999). Over a two-day period in October 2016, 32 to 51 mm fell in the vicinity of Hurghada, causing extensive flooding that extended northwards to Ras Gharib where according to a media report by the Ministry of Irrigation and Land Reclamation the combined runoff volume from several wadis reached 120 x 10^6 m^3. In a 55-year rainfall record comparable quantities were recorded only once at Qena (57 mm in 1949) and once at Quesir (60 mm in 1965) (Nicholson, 1997). At Quseir, to the south of the study area, the irregular rainfall regimen is marked by long, almost completely dry periods, which are interrupted by rare, high-magnitude events (Nicholson, 1997). In 1989, 1994 –1997 and 2010, in particular, winter rains around Quseir and Hurghada were significant and runoff scoured the wadi beds (Moeyersons *et al*., 1999; El-Sawy, Bekheit, Abd El-Motaal, Orabi, Abd El Gany, 2011) and damaged infrastructure (Yehia *et al*., 1999; Faid, 2009). From consideration of coastal and other lowland rain gauges, Gheith & Sultan (2002) suggested major localized Eastern Desert floods occur as frequently as every 40 months. With respect to high elevations, the only available data is for the Sinai Jebel Katherine (2629 m) for which Abd-Elhamid *et al*. (2018) calculated rainstorm durations and intensities. The nearest evaporation data are available for Wadi Qena (6.2 mm day^{-1}) (Abdel-Fattah *et al*., 2017) west of the Red Sea Mountains, whereas for wadis southeast of the study area, Abdalla *et al*. (2014) reported annual evaporation rates equivalent to the annual rainfall, akin to detailed records in the Gulf of Eilat (Ben-Sasson, Brenner, Paldor, 2009).

Hobbs (1990) compiled the occurrence of wetter periods and droughts in the northeastern areas of the desert from oral Bedouin tradition and published accounts.

Wet periods: 1887; 1926-32; 1951-52; 1955; 1960-61; 1968-70; 1987-88.

Droughts: 1870-73; 1882-86; 1928-32; 1949-51; 1956-58; 1977-85; 1980-85,

with a notable lengthy dry period from 1943-58. The occurrence of conflicting dates within this record reflects the fact that the individual records rarely relate to regionally-extensive hydrological events, but rather more localised flooding. Nonetheless, it is evident that wetter periods usually last only a couple of years whereas droughts can last considerably longer.

Winters bring occasional light rainfall (Aggour & Sadak, 2001) associated with low cloud over the mountains and rare snow may fall at high altitudes. In the summer, the mountains are subject to infrequent, intense convective rainstorms lasting no more than one or two hours, effecting local catchments rather than being regional in extent. Although there are numerous passing records of individual catchments being subject to flash flooding (*e.g.* Tregenza, 1955; Labib, 1981; Hobbs, 1990; Elsadek *et al*., 2018), these reports lack detail of flood wave characteristics and progression. Recent attempts to model wadi floods suggest time to peak can be as short as 8 hours in upstream locations to 17 hours nearer the coast (Sumi et al., 2013).

Extensive regional flooding, such as occurred in 1954 and 1975 to the west around Wadi Qena (area ~ 16,000 km^2), that drains to the Nile, is relatively infrequent (Kassas & Girgis, 1964; Labib, 1981; Hobbs, 1990). Other floods occurred in Wadi Qena in 1987, 1994, 1997, 2010, 2014, 2016 (Abdel-Fattah *et al*., 2017; Moawad, Abdel Aziz, Mamtimin, 2018) but not on the scale of the 1954 event, which also affected the east of the region. Flooding tends to be recorded officially only in those cases where the coastal infrastructure or Qena city is affected (El-Sawy *et al*., 2011). Media reports include major flooding in January 2010, March 2014, and October 2016 in Hurghada from rainfall that was regional in extent. Thus, large floods may be defined qualitatively as those that reach Qena in the west, or the east coast. Clearly, these latter floods have sufficient volume to exceed the infiltration capacity of the wadi beds and feed coastal aquifers.

Extensive coastal flooding requires exceptional precipitation in the mountains (examples occurred in 1969, 1980, 1984, 1985, and 1994; Moneim, 2005). In the case of the November 1994 regional event (recurrence interval ~ 40 months), for example, initial transmission losses were 21 to 31 % and only 3 to 7 % of the runoff reached the coast (Gheith & Sultan, 2002; Abdel-Fattah et al., 2017). Such large floods are related to synoptic weather systems. In October, a low-pressure trough (the Red Sea Trough) can penetrate the region as an extension of the African Monsoon, giving rise to heavy but usually localised rainfall (Dayan *et al*., 2001). From December through to March the North Atlantic Oscillation can affect the Levant (Cullen, Kaplan, Arkain, Damenocal, 2002; Eshel & Farrell, 2000) giving rise to precipitation that is widely distributed. Localized convective rainfall is often triggered by orographic effects and any resultant small floods are typically confined within the upper reaches of the wadis; high transmission losses then prevent most floods reaching the coastal plain. As noted above, evaporation rates are high and infiltration rates range between 1.33 mm day^{-1} to 8.18 mm day^{-1} (Ismail, Othman, Abd El-Latif, Ahmed, 2010), which are typical values for sandy-loams and sands.

Abdalla *et al*., (2014) suggested that flash-flood frequency in the wadis south of Quseir has increased from an event every 9 years to an event every 6 years, possibly due to climate change. In the neighbouring hyperarid Gulf of Aqaba region, an exceptional number of flash floods reached the gulf during the winter of 2012–13 (Katz *et al*., 2015). In that case, high quantities of flood sediment impacted coral reefs and promoted hyperpycnal flows that extended to the deep offshore basins. Thus, in similar vein, flash floods from the Eastern

Desert that reach occasionally to the Red Sea impact infrastructure and possibly also the marine environment. However, there is little information on sediment yield from the wadis (Labib, 1981), flood routing and the impact on coastal infrastructure. Perception of flood risk may be growing either due to an increased frequency of flooding in recent years, or due to the increase in flood-damage and lives lost that are related to rapid urbanization of an area that was previously sparsely-inhabited. In this context, Abd-Elhamid *et al*. (2018) examined the flood risk for Hurghada and the coastal highway from runoff generated in small basins along the coastal strip; however, they neglected the possibility of even greater floods sourced from the Red Sea Mountains further inland. Nonetheless, efforts to model flood risk in the broader region are increasing mainly via distributed GIS-based hydrological models (El-Magd *et al*., 2010; Moawad, 2012; 2013; El-Sawy *et al*., 2014; Gabr & El Bastawesy, 2015; Farhan and Anaba, 2016) as well as using boulder competence equations (Kehew *et al*., 2010; Greenbaum *et al*., 2020). Such models are yet to be calibrated with locally-derived hydrological data.

3. Study Area

Geologic setting

Wadi Umm Sidr drains rugged terrain with up to ~ 1300 m relief in the Red Sea Mountains (Figs. 1 and 2A)—the uplifted western flank of the Red Sea rift (Said, 1990). The bedrock-confined wadi and catchment is cut in Neoproterozoic Dokhan volcanics, with both granite and granodiorite-quartz diorite flanking the wadi at the rangefront (Eliwa, Kimura, Itaya, 2006). Andesitic and dacitic lavas, less abundant tuff and agglomerates are also reported (Makovicky, Frei, Karup-Møller, Bailey, 2016). The agglomerates are the Hammamat Group, a sequence of immature, clastic sedimentary rocks that crop out sporadically in the region, although their distribution in the study area is known imperfectly.

A general geomorphological context of the region is provided by Said (1990). The tightly bedrock-confined (~ 40–200 m width) mainstem of Wadi Umm Sidr (Fig.3A) is essentially linear, trending west-of-north to east-of-north, the alignment being fault-controlled as the valleys typically trace multiple parallel faults. Subsidiary faults aligned northwest-southeast (Said, 1990) also mediate valley alignment. The major right-bank tributary, Wadi Abu Ma’amel (Figs. 2A; 3B), is fault-aligned slightly west-of-north.

Colluvial aprons truncated by the channel have left terrace-like remnants, but unlike Wadi Gattar in the neighbouring Jebel Gattar granite massif, we observed no alluvial terraces in Wadi Umm Sidr. The surface bed-sediments of the mainstem Wadi Umm Sidr comprise primarily sand and rounded pebbles and small cobbles. Tributaries, including Wadi Abu Ma’amel, are lined with coarser bed-sediments mainly large cobbles and small boulders. This coarser gravel fill terminates abruptly where tributaries meet the generally sandy mainstem, presumably reflecting a reduction in flow competence (Fig 3A). We did not observe bedrock exposed in the channel bed between Mons Porphyrites and the rangefront (Fig. 2A), suggesting the alluvium hosts a thin aquifer above bedrock. The thickness of alluvial fill available for recharge is not known. A Roman well (27.2582° N, 33.3013° E) in a minor tributary of Wadi Abu Ma’amel (Fig. 2A) is reported to be 11.6 m deep (Fig. 3E) and another well (27.2510° N, 33.3000° E) in the centre of the Ma’amel channel, 6.7 m deep (Wilkinson, 1832); both floored by bedrock. A further rangefront well (27.0891° N, 33.2290° E) is ~ 19 m deep in Wadi Gattar. Such depths are less than those reported from three other wells (~ 20 m, > 20 m, ~ 40 m) in bedrock-confined wadis elsewhere in the region (Tregenza, 1955; pp 39, 52, 187). Alluvial fills in unconfined wadis nearer the coast can be 100–200 m thick (Abdalla *et al*., 2016), but it seems that bedrock-confined wadis support a shallow ground water system floored by largely impervious bedrock at no great depth.

Figure 3: (A) View of Wadi Umm Sidr sandy bed to the left of the 4WD vehicle at the junction with Wadi Abu Ma'amel, which enters from right to left. Coarser, dark-hued, small boulder and cobble gravel characterizes the Abu Ma'amel bed materials; (B) View of Wadi Abu Ma'amel rocky bed looking downstream width of channel > 200m; (C) Ruined stone columns surrounding Roman well at Lykabettos in Wadi Ma'amel, flow left to right; (D) View looking east into the gorge of Wadi Beli'; (E) Roman well showing >11m thick shallow aquifer gravels above bedrock In Wadi Ma'mel'. (F) Example of 2017 flood deposited sand (right) above coarse angular dark-hue slope-washed gravels along right-bank of Wadi Sidr - horizontal field of view in foreground c. 2m.

Surface hydrology of Wadi Umm Sidr

Wadi Umm Sidr is the largest catchment (103 km^2) draining this part of the Red Sea Mountains. Although there are no rain gauges within the catchment, estimates of annual rainfall distribution (Fig. 2B) according to the WorldClim dataset (Fick & Hijmans, 2017) are possible via spatial interpolation from coastal and Nile valley data. These estimates indicate mean annual rainfall of ~ 10 mm over the period 1970–2000. Such an assessment is in accord with the sparse regional rainfall records (Gheith & Sultan, 2002), which suggest an important orographic component to local rainfall (Fig. 2B). Floods capable of reaching the rangefront, or indeed the coast, would require a rainstorm of well in excess of the mean annual total.

A ruin of a rock-walled Roman way-station (27.2962° N, 33.2966° E) located in the centre of the wadi has an upstream channel-transverse wall several metres thick, seemingly constructed to protect the station from flash floods—perhaps indicating such floods threatened infrastructure, as today. The Romans established a village—Lykabettos—on the right flank of Wadi Abu Ma'amel (Fig. 2A) adjacent to the extensive Mons Porphyrites stone quarry. The Roman settlement declined in the 4th century AD and was abandoned in the mid-5th century (Del Bufalo, 2004). In the wadi bed near the village, four Roman masonry pillars (Fig. 3C), which surround a sediment-filled well (27.2510° N, 33.3000° E), have withstood the passage of floods for at least 1500 years. However, a flood in 1996 destroyed part of the rock-paved Roman road near the village (Del Bufalo, 2004) and so this recent flood may represent the largest along Wadi Abu Ma'amel since Roman times. Floods sourced from Wadi Umm Sidr can reach the coast if augmented by discharge from Wadi Bali'. Such floods reached Hurghada on 9 March 2014 and 27 to 28th October 2016 via Wadi Bali' gorge (Figs. 2A; 3D). Local opinion is that Wadi Bali' floods every ~ 5 years, with rarer occurrence nearer the coast where flood depths can be ~ 0.5–1 m.

According to the local Khushmaan Bedouin leader, Sheikh Abdul Zahir, who has visited Wadi Umm Sidr regularly, there was minor but reliable runoff in the upper mainstem most years from the 1940s to 1983, with an exceptional flood in 1954, as reported for Qena above. A drought lasted 11 years from 1983. Since 1954, around five large floods have occurred, most recently in 1996, 2010, 2014 and 2016. Visual evidence of rain falling on Jebel Abu Dokhan (Fig. 2A) is generally expected to be followed by surface runoff an hour later in Wadi Umm Sidr ~ 9 km downstream of the catchment head. Such anecdotal information is imprecise but indicates that: (i) small flows in the upper wadi occur in most years; (ii) large floods previously had a roughly decadal occurrence and are possibly becoming more frequent; (iii) only rare large floods reach the coast; and (iv) the rainfall-channel flow lag time in the upper catchment is a matter of a few hours only.

4. Methods

Peak discharge estimation

In 2017, four cross-sections (numbered in a downstream direction) within Wadi Umm Sidr and three cross-sections within Wadi Abu Ma'amel were surveyed with a theodolite (Fig. 2A) in straight reaches where the bed was relatively uniform and valley sidewalls were well-defined. As flood debris is usually deposited slightly below maximum floodstage, debris heights were surveyed along flow margins. In the case of Wadi Umm Sidr, two insignificant left-bank tributaries enter the mainstem within the surveyed reach (between sections 1–2 and 3–4, respectively). In the case of Wadi Abu Ma'amel there were no tributary influences (Fig. 2A). Bed slopes were determined from a longitudinal channel profile devised from the Shuttle Radar Topographic Mission 1 arc-sec digital elevation model.

Estimates of peak discharge, Q_p, were obtained using HEC-RAS 4.1 (Hydrological Engineering Center, 1998) by calculating water-surface profiles for steady flow, as is appropriate using the one-dimensional energy equation. Energy losses were evaluated by selecting a range of energy loss coefficients (Manning's *n*) with the channel contractionexpansion coefficient set by default as no major changes in section occurred along the study reaches. A range of Manning's *n* values: 0.02, 0.04, 0.06 and 0.08 (s $m^{-1/3}$) was trialled to accommodate all likely roughness scenarios of shallow flow over a rough bed. Applying reach-scale mean bed slope (S = 0.014 in Sidr, S = 0.021 in Ma'amel) and a range of hydraulic radii (R = 0.5, 1.0, and 2.0 m) in the Jarrett (1984) bed roughness estimator ($n = 0.32\ S^{0.38}\ R^{-0.16}$) suggests that appropriate Manning's *n* values might lie towards the upper end of the trial range (n = 0.057–0.071 in Sidr, n = 0.067–0.083 in Ma'amel).

Eight flood profiles were explored with Q_p values: 250–600 $m^3\ s^{-1}$ (in 50 $m^3\ s^{-1}$ increments) for either subcritical or mixed-regime settings. A similar approach was used for the Wadi Abu Ma'amel sites upstream with Q_p values in the range: 150–450 $m^3\ s^{-1}$. The initial reach boundary conditions were the known minimum water surface elevations indicated by flood-debris, mean bed slope, normal depth, and critical flow depth. Finally, the Q_p estimate for Wadi Umm Sidr was used to calculate the approximate total volume of the flood wave using data for floods in the hyperarid Negev (Greenbaum, 2002), the most comprehensive assessment of wadi hydrology in the Levant:

$$Q_{vol} = 14054\ Q_p^{1.05} \qquad (1)$$

Samples of recent suspended sediment deposited along the channel margins and of recent bedload transport from the channel centre were sized at 0.25 Φ intervals using a laser Malvern Mastersizer 3000 for particle sizes < 3 mm. Particles > 1 mm were sieved. The laser and sieve size distributions were combined, and statistics calculated to assist in selecting values of hydraulic conductivity.

Infiltration and aquifer recharge

The initial consideration is the theoretical infiltration rate expected at the channel bed. The Green-Ampt infiltration equation (Huang *et al*., 2015) was used to determine the probable infiltration rate (*f*):

$$f = \frac{dF}{dt} = K_s \left[1 + \frac{(\theta_{s-}\theta_i)H_c}{F}\right] \quad (2),$$

where θ_s = 1 is the saturated volumetric water content and θ_i = 0.1 is the initial (dry bed) volumetric water content, and H_c (2 m) is the maximum hydraulic head. The saturated hydraulic conductivity K_s, is estimated for sandy-gravel deposits (d_{10} = 0.03 m) using the procedure of Chapuis (2004; his Eq. 17) and *F* is obtained iteratively, where *t* is the period of flooding considered:

$$F = K_s t + H_c \ln\left(1 + \frac{F}{H_c\,(\theta_{s-}\theta_i)}\right) \quad (3).$$

The observed infiltration rate was estimated using the procedure presented by Greenbaum (2002) based on the field measured flood parameters and the water balance in the study catchment:

$$ft = [Qvol_1 - Qvol_2(x, w)] \quad (4)$$

where *t* is the duration of flow, $Qvol_1$ is the total flood volume at the upstream reach, $Qvol_2$ is the total flood volume at the downstream reach mediated by the distance between the reaches (*x*) and the breadth (*y*) of the flow. Parameter values for $Qvol_1$ and $Qvol_2$ were obtained from Eq. 1 and *t* is estimated following Greenbaum (2002).

5. Results

General observations

Fresh, light-coloured very fine to medium sand (*D_{50}* = 66 to 250 μm) deposits surveyed in 2017 represent suspended sediment deposited along the channel margins by a small flood subsequent to the major 2016 event. This flood also transported a fine bedload in the main channel (*D_{50}* = 1.5 mm with some grains ~ 10 mm); however, the coarser bed sediments such as medium-sized pebbles and cobbles do not seem to have been mobilized. Higher, well-defined lines of debris composed of dry vegetation ~ 1–2 m above the channel low points have low preservation potential and point to the major 2016 event. The debris lines are at the same elevation as dark-coloured, lightly-weathered sandy deposits that might be attributed to the 1996, 2010, 2014 or 2016 floods (Figs. 3F, 4 and 5). Such deposits from large floods often are preserved in marginal locations along dryland rivers, where they are termed 'slackwater' deposits (*e.g.* Greenbaum *et al*., 2020). Sections cut into these slackwater deposits sometimes showed two layers separated by a thin bioturbated layer. The lower layer thus pre-dates the 2016 sand layer and may represent the 2014 or the other most recent floods.

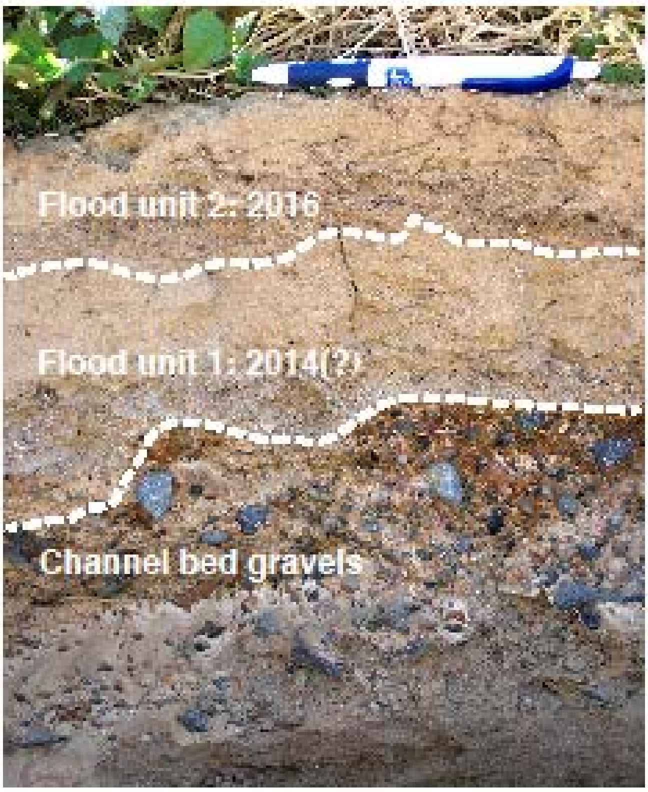

Figure 4: Undated slackwater deposits at margin of Wadi Umm Sidr. Basal unit of channel gravel scoured by recent floods. Flood unit 1 consists of granules at the base topped by fine sands. Flood unit 2 consists of coarse sand at the base (with some evidence of bioturbation) topped by fine sands. Pen for scale, 15 cm in length.

Wadi Umm Sidr peak flood estimations

Considering our four cross-sections on Wadi Umm Sidr (Fig. 5), HEC-RAS runs with n = 0.02 yielded Froude numbers, Fr >>1 and extremely high velocities, which are unreasonable and consequently excluded. Selecting subcritical or mixed regime affected only the extreme n = 0.02 runs, which suggests that subcritical flows (perhaps approaching critical) mostly prevail at peak floodstage. By using a reach-boundary conditioned by the 'known water surface' linked to the debris and assuming subcritical flow, we sought to simulate close to critical water-surface elevations that equalled or slightly exceeded the level of flood debris. The Jarrett (1984) equation suggested solutions in the range, n = 0.057 to 0.071, so these initial observations cover a range of possible Q_p values. Figure 6 depicts the HEC-RAS output for Q_p = 500 $m^3\ s^{-1}$ with n = 0.06 and n = 0.08 bracketing the Jarret (1984) approximation. For such a flood, the Greenbaum (2002) approach predicted a complete flood cycle of ~ 50 hours, with a total flood volume, $Qvol_1$ ~ 9.59 x 10^6 m^3. We return to the question of peak flood discharge in the Discussion below.

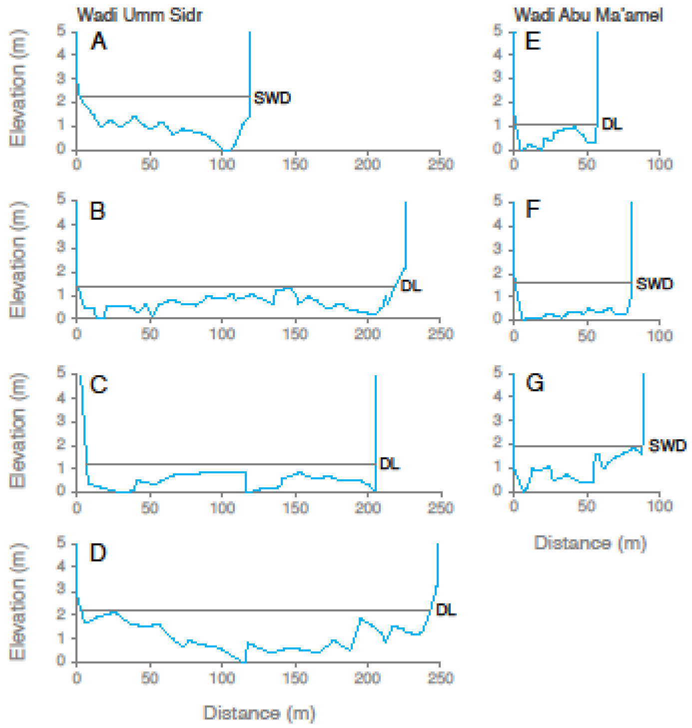

Figure 5: Valley cross-sections used in our HEC-RAS modelling (upstream to downstream). Water levels are defined by flood debris (arrows).

Wadi Abu Ma'amel peak flood estimations

Considering our three cross-sections on the tributary, Wadi Abu Ma'amel (Fig. 5), the HEC-RAS runs were subject to the same limitations as those outlined above for Wadi Umm Sidr. The Jarrett (1984) equation suggested solutions in the range, n = 0.067 to 0.083. Acceptable simulations returned Q_p ~ 100–150 m^3s^{-1}. The lower limit provided critical water-surface simulations above but closer to the debris levels relative to the upper limit. Again, we return to the question of peak flood discharge in the Discussion below.

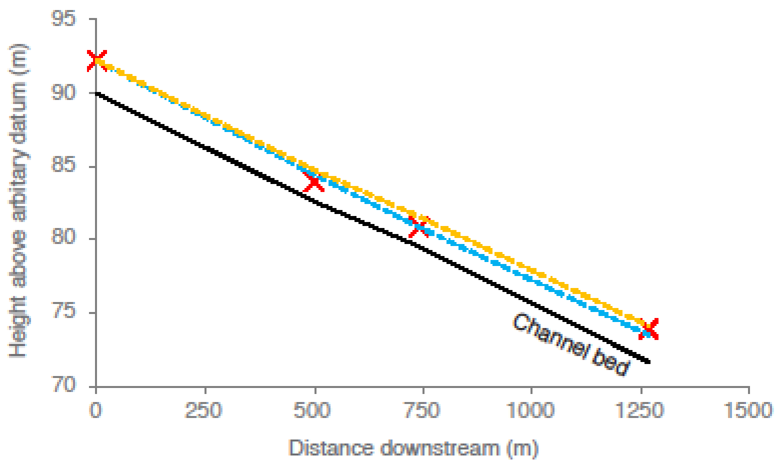

Figure 6: Example of water surface profiles predicted by HEC-RAS for the 2016 flood in Wadi Umm Sidr. Red crosses: Observed trashlines; Black curve: Channel bed elevation; Blue curve: Q_p= 500 m^3s^{-1}, Subcritical Flow, n = 0.06; Brown curve: Q_p= 500 m^3s^{-1}, Subcritical Flow, n = 0.08.

Wadi Bali' peak flood estimation

The 2016 flood reached the Red Sea coast via Wadi Bali' (Figs. 2A; 3D). We observed debris lines standing 1.0–1.5 m-high in the gorge near the coast (27.3888° N, 33.5534° E) putatively from 2016 but we could not survey them. We also noted the bed (width, *w* = 80 m) displayed degraded antidunes with a wavelength of ~ 2.5 to 3.2 m. An average 3 m wavelength relates to a mean velocity ($\overline{U}$) of 3 m s^{-1} and depth (*h*) of 0.48 m (Allen, 1982); the latter consistent with bedform development on the falling stage. Considering continuity ($Q_p = \overline{U}hw$), we can estimate mean velocity ≤ 3 m s^{-1} and maximum depth ~ 1.5 m during peak flow. Therefore, given an 80 m-wide channel, a crude Q_p estimate for the 2016 flood in lower Wadi Bali' is ≤ 360 m^3 s^{-1}. Corresponding to this flood, the Greenbaum (2002) approach (Eq. 1) yields a total downstream flood volume, $Qvol_2$ ~ 6.79 x 10^6 m^3.

Wadi Umm Sidr infiltration estimations

In a study by Gheith & Sultan (2002) of the Eastern Desert, it was found that evaporation losses were negligible given the short duration of floods and the usual cloudy weather associated with regional storm events. Hence the presumably minor role of evaporation is not considered in the present study. The rock-walled channels (Figs. 3A and 5) limit the contact between the alluvial bed and the water mass, and the shallow alluvial fill has limited capacity to store infiltrating water. However, where alluvial fills deepen beyond the rangefront flows should experience high transmission losses to substrate aquifers.

Values for the theoretically expected infiltration rate, f, can be obtained by varying Equation 2 parameter values within reasonable ranges. Selected parameter values are: the porosity of the arid channel sandy bed, $\Theta_s = 0.33$ (Schwartz & Schick, 1990); the initial 'dry' water content, $\Theta_s = 5$ % (Yair & Danin, 1980); the saturated hydraulic conductivity, $k_s = 0.038$ m s^{-1} for a gravel-bed grain size, $d_{10} = 0.03$ m (Chapuis, 2004). For example, after 3 hours of flooding, $f = 3.28$ m day^{-1} and at the end of the flood (50 hours), $f = 1.19$ m day^{-1}. These values fall within the lower end of the range of the Eastern Desert infiltration rates reported above by Ismail et al. (2010).

Values for the observed infiltration rate, f in Equation 4, can be obtained for the 2016 flood for comparison with theory (Eq. 2). The distance, $x = 23$ km, is measured between the rangefront and the Wadi Bali' gorge near the coast. The total flood volumes ($Qvol_1$ and $Qvol_2$) for the reach within Wadi Umm Sidr and at the Wadi Bali' gorge are given in sections above. Channel width (w) downstream of the rangefront is not known, but for $w = 80$ m (i.e., the width of Wadi Bali' gorge), after 20 hours of flooding, $f = 1.82$ m day^{-1}, which is consistent with the theoretical derivations. Nonetheless, observations of the braiding river pattern point to active channel belts above the Wadi Bali' gorge of up to 500 m wide. Based on Equation 4, it can be said that infiltration rates are likely to be substantially greater than 1 m day^{-1} for wider channels.

6. Discussion

Wadi Umm Sidr peak flood estimation within a regional context

Our HEC-RAS modelling estimates of peak discharge come with considerable uncertainties—not least because the propagation of the flood wave is unsteady, though it probably varies gradually around the flood peak. More significantly, the high width-depth ratio of the Umm Sidr floods produces hydraulically heterogeneous and highly turbulent conditions. The selection of appropriate energy slope and bed roughness is therefore challenging, and such properties are likely to vary considerably over short distances. Consequently, we anticipate > 50 % uncertainty in our Q_p estimates.

Despite these limitations, we can apply some useful constraints that build on previous studies. Reid *et al*. (1995) reported measurements from large floods along Nahal Yatir, a steep channel in the hyperarid Negev, with Manning's *n* consistently ~ 0.07 (1 σ = 0.003, n = 9) and mean velocity ~ 2 m s^{-1}. These values support the higher-end Jarrett (1984) roughness estimations for Q_p in Wadi Umm Sidr ~ 300–600 m^3 s^{-1}. Our results for *n* = 0.02 yielded excessive velocities and Froude numbers, while for *n* = 0.08, velocities and Froude numbers mostly were unacceptably low. Hence, we excluded *n* = 0.02 and retained *n* = 0.04–0.08 as lower and upper limits, respectively.

Grant (1997) has suggested that in steep bedrock-constrained channels with alluvial fill, rising flood flows asymptotically approach a limiting state of *Fr* = 1. This critical flow condition concurs with observations of Greenbaum *et al*. (2001) that supercritical flow is rarely observed in Negev wadi floods. An increase in Manning's *n* occurs towards peak flow (Grant, 1997) at which stage critical flow depth should be somewhat higher than the observed debris-indicated water depth (Greenbaum *et al*., 2001). Adopting a conservative criterion in which modelled critical flow should be slightly higher than the observed debris-line flood levels, 29 of our simulations for $0.04 \leq n \leq 0.08$ predict Q_p around 500 m^3 s^{-1} or slightly higher.

The estimated Q_p of 500 m^3 s^{-1} for the 2016 Umm Sidr flood is reasonable, yielding a unit-area discharge of 4.85 m^3 s^{-1} km^{-2}. Judging from stratigraphic evidence (Fig. 4), the 2016 and 2014 (or possibly 1999) floods were of similar magnitude and the occurrence of two large floods in quick succession is unlikely to be rare. Given its headwater setting, the unit-area discharge relationship for the Wadi Abu Ma'amel site is likely to be similar or somewhat greater than for Umm Sidr downstream. Our modelling results show that an Abu Ma'amel peak discharge of 150 m^3 s^{-1} is plausible, but we are more confident with Q_p = 100 m^3 s^{-1}, yielding a unit-area discharge of 8 m^3 s^{-1} km^{-2}. To give some broader context, we plot the 2016 Umm Sidr and Abu Ma'amal flood estimates among reliable flood data compiled from comparable hyperarid sites in the southern Levant (Fig. 7). The 2016 flood falls within the envelope curve for modern Negev floods recorded up to 2004. Also shown are the only previous Q_p estimates from the Eastern Desert, 104 m^3 s^{-1} (El-Magd *et al*., 2010), and the Sinai peninsula, 240 m^3 s^{-1} (Cools *et al*., 2012) and 2864 m^3 s^{-1} (Sumi *et al*., 2013) — none of which are field-based studies. The El-Magd *et al*. (2010) flood estimate is probably too high due to channel roughness underestimation (Manning's n = 0.02). The Sumi *et al*. (2013) Q_p estimate (which plots above the (b) and (c) envelope curves) was developed using the rainfall-runoff procedure, HydroBEAM. Both this Q_p estimate and that of Cools *et al*. (2012) may also be too high, as explained in the next section.

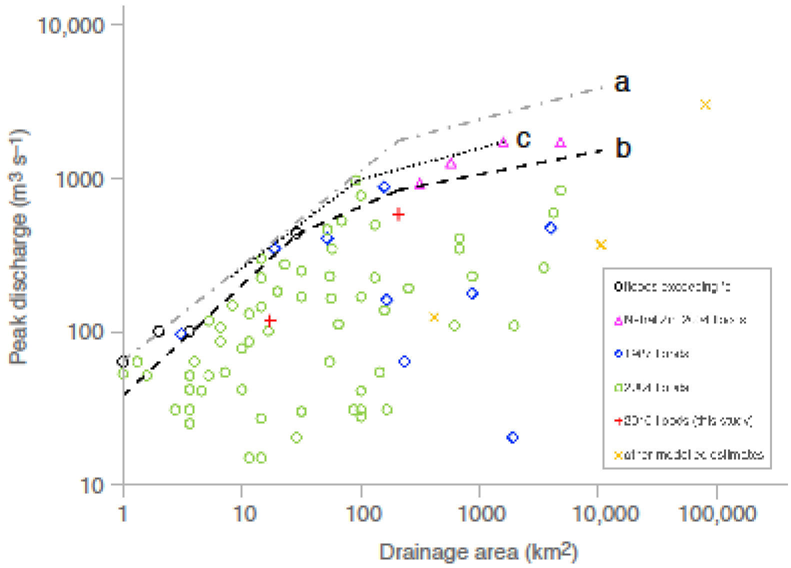

Figure 7: Compilation of field-measured and modelled Q_p estimates for hyperarid catchments in the Negev (N) and Dead Sea (DS) regions (redrawn from Greenbaum et al., 2010). Envelope curve (a) represents the Negev palaeoflood record; (b) represents the Negev field-measured record prior to 2004; (c) represents the Dead Sea field-measured record after 2004.

Wadi Umm Sidr total flow estimation and the regional context

Owing to the absence of flow gauge data for the Eastern Desert, previous studies have relied upon modelled rainfall-runoff relationships to estimate *Qvol* from Q_p. Sumi *et al*. (2013) and Abdell-Fattah *et al*. (2017) made use of the HydroBEAM runoff model, whereas Gabr & Bastawesy (2015) used a bespoke GIS-based model. In all cases, models were uncalibrated and runoff coefficients were estimated. The results of these three independent studies (Fig. 8) demonstrate a remarkable consistency in terms of a near monotonic increase in *Qvol* with Q_p (for all three datasets combined, $Qvol = 119425\ Q_p^{0.9961}$). The trend of HydroBEAM model estimates parallels a similar function for Nahal Zin in the hyperarid Negev (Fig. 8); however, the latter is derived from a large empirical dataset (1935–1998; Greenbaum, Schwartz, Bergman, 2010). The estimated runoff coefficients used in HydroBEAM predict floods that are an order of magnitude greater than those observed in Nahal Zin. Given that the Eastern Desert and Negev are both hyperarid regions, the parallel trends suggest that the HydroBEAM model structure is correct by and large, yet the total runoff and hence potential aquifer recharge may be overestimated.

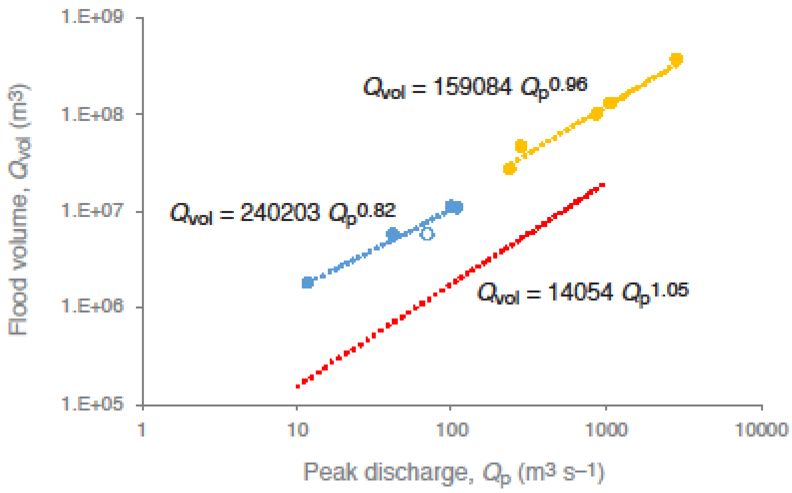

Figure 8: Relationship between flood volume (Qvol) and peak discharge (Q_p) for sites in the Eastern Desert (Abdel Fattah et al., 2017, blue dots; Sumi et al., 2013, yellow dots) and Sinai (Gabr and Bastawesy, 2015; grey dot), and the Negev's Nahal Zin (Greenbaum et al., 2010, red dotted line).

Infiltration

Zaid (2009) applied the distributed runoff model of El Shamy (1992) to four catchments inland from Quesir that are broadly similar to Wadi Umm Sidr. The analysis demonstrated that the four catchments fell within El Shamy's *Domain C*, wherein low to moderate infiltration is expected (15 % of runoff) and thus relatively moderate to high flood risk. Despite using a range of catchment sizes (135 to 1645 km^2), including upland and coastal plain sites, Zaid reported a uniform infiltration rate — inviting some caution. A more reliable approach is that of Gheith & Sultan (2002) who employed the US Department of Agriculture-Natural Resources Conservation Service method to estimate water balances for catchments on the western slopes of the Red Sea Mountains. Using expressions developed for hyperarid southwestern Saudi Arabia, Gheith and Sultan reported transmission losses and groundwater recharge rates — estimating that during the 1994 flood event, groundwater recharge via transmission losses ranged from 21 to 31 % of the flood volume.

In our analysis of Wadi Umm Sidr, we estimate the volume lost to infiltration between $Qvol_1$ and $Qvol_2$ at ~ 2.80 x 10^6 m^3 (7153 m^3 h^{-1} km^{-2} over a transport distance of 23 km during the initial 17 hours of the flood). This result is consistent with transmission losses (Ben-Zvi, 1996) reported for Negev wadis, typically ~ 7200 m^3 h^{-1} km^{-2}. Transmission loss between the rangefront and the Wadi Bali' gorge is ~ 30 % of the upstream flood volume. Similarly, Shentsis, Meirovich, Ben-Zvi, Eliyahu Rosenthal, (1999) analysed runoff data for Wadi Tabalah, Saudi Arabia, where transmission losses were consistently ~ 30 % of the upstream flood volume over a distance of 24 km. The comparable results of Gheith & Sultan (2002) are noted above. Aquifer recharge is dependent on the frequency of flooding, which remains to be determined for Wadi Umm Sidr, but it does appear that significant quantities of flood water extended across the coastal plain aquifer during the 2016 (and 1996 to 2014) flood and infiltration was significant. This observation appears contrary to the judgement expressed by Moneim (2005) that the catchments west of Hurghada have relatively low aquifer recharge potential. However, until reliable flood-frequency data are assembled, the long-term recharge cannot be assessed. It is clearly true that major floods occasionally reach the lower course of Wadi Bali' and hence Moneim (2005) was correct to assert that a high flash-flood risk extends to the coast.

7. Summary and future directions

Although limited empirical data are available to define the flood dynamics and aquifer recharge potential of Wadi Umm Sidr, and considerable uncertainty exists regarding appropriate hydrological parameters, we have attempted to build upon data from comparable and better-quantified hyperarid catchments in the southern Levant.

The transmission losses estimated here (~ 30 %) govern the passage of floodwaters downstream and, in turn, are dependent upon the duration floodwaters spend across substrates of differing permeability. The magnitude, shape and time-base of any given flood hydrograph is best studied by monitoring the progression of actual flood waves in the field or by remote sensing. However, useful insights can also be gained by field survey of recent floods, as outlined below.

The absence of rainfall and streamflow gauges in the Eastern Desert is a major impediment to understanding the surface and subsurface hydrology. As a first step, we foresee great value in a systematic field survey of recent flood debris (and palaeoflood indicators) along wadis in the region. Using flood debris to map the passage of floods during the past decade or more at sequential locations downstream over a range of drainage areas would enable calculation of regional unit-area discharge relationships. Such information would provide direct insights to aquifer recharge potential and flood risk to coastal settlements. Remote sensing of runoff events across the entire Eastern Desert is possible and would permit development of a database recording the magnitude and frequency of modern discharge events at singular locations. Dating ancient flood deposits and palaeohydrological analysis would then extend the modern flood record to build a regional understanding of flood magnitude-frequency relationships in the Eastern Desert over the past several thousand years, potentially.

The estimated peak discharge of ~ 500 $m^3\ s^{-1}$ for the 2016 Wadi Umm Sidr flood, together with the large floods in 2014, 2010 and 1996, indicate that construction of earthen impoundments in the larger wadis, such as Umm Sidr, may pose unforeseen and unquantified flood risk to coastal settlements. Such in-stream structures have been proposed by some prior studies (Abdalla *et al*., 2014; Abd-Elhamid et al., 2018) as a means to protect the coast from large floods; however, these studies did not appreciate the flood volumes involved. As shown by experience elsewhere, earthen impoundments are at high risk of failure when faced with large volume, high velocity floods (Chongxun *et al*., 2008). Dam failure could trigger catastrophic consequences for people and coastal infrastructure. Rather, we suggest diversion bunds should be designed (Stephens, 2010) in the lower water courses to slow the flow (Abdalla *et al*., 2014) and channel floodwaters away from infrastructure. In addition, many coastal roads may not be fitted with adequate culverts or bridges to allow floodwaters to pass. Adequate flood passage should be accommodated by future designs. In some areas, we noted recent urbanization extending into potential floodways, suggesting that development zoning is not effectively accounting for the inevitable passage of floodwaters to coastal outlets. In this manner, unimpeded floodwaters can recharge coastal aquifers without damage to infrastructure.

Acknowledgements

PAC was supported by grant-in-aid from the Council for British Research in the Levant and through provision of a Royal Geographical Society Thesiger-Oman Fellowship. JDJ was supported by the Danish Council for Independent Research under grant number DFF-6108-00226. We acknowledge the Traditional Owners of the Eastern Desert lands and thank Sheikh Abdul Zahir, Samira Ouda, and Pierre-André Jean Denereaz of the Desert Life Company for their hospitality and logistical assistance during fieldwork. Jamie Woodward is thanked for positive comments and suggestions for revisions related to the original submission.

Competing interest statement

The authors have no competing interests to declare.

Disclosure statement

No financial interest or benefit has arisen for the authors with respect to the direct applications of the research reported herein.

Data Availability Statement

Data used in the preparation of this article are available from the corresponding author.

References

1. Abdalla, M.A., Mekhemer, H.M., Abdallah Mabrou, W., 2016. The hydrogeological conditions in Sahel Hasheesh, Eastern Desert, Egypt. *National Research Institute of Astronomy and Geophysics*, **5**: 238-246.
2. Abdalla, F., El Shamy, I., Bamousa, A.O., Mansour, A., Mohamed, A., Tahoon, M., 2014. Flash floods and groundwater recharge potentials in arid land alluvial basins, southern Red Sea coast, Egypt. *International Journal of Geosciences*, **5**: 971-982.
3. Abdel-Fattah, M., Saber, M., Kantoush, S.A., Khalil, M.F., Sumi, T., Sefelnasr, A.M., 2017. A hydrological and geomorphometric approach to understanding the generation of wadi flash floods. *Water*, **9**: 27pp.
4. Abdel-Lattif, A. and Sherief, Y., 2012. Morphometric analysis and flash floods of Wadi Sudr and Wadi Wardan, Gulf of Suez, Egypt: using digital elevation model. *Arabian Journal of Geosciences*, **5:** 181-195.
5. Abd-Elhamid, H.F., Ismail Fathy, I., Zeleňáková, M. 2018. Flood prediction and mitigation in coastal tourism areas, a case study: Hurghada, Egypt. *Natural Hazards*, **93:** 559–576.
6. Aggour, T.A. and Sadek, M.A., 2001. The recharge mechanism of some cases of the different groundwater aquifers, eastern Desert, Egypt. *Bulletin of the Faculty of Science, Mansoura University*, **28**: 43–78.
7. Allen, J.R.L., 1982. *Sedimentary Structures: Their Character and Physical Basis*. Vol. 1. Elsevier, Amsterdam, 593pp.
8. Ben-Zvi, A., 1996. Quantitative prediction of runoff events. pp. 121-130 In: Issar, A.S., Resnick, S.D. (Eds.). Runoff, Infiltration, and Subsurface Flow of Water in Arid and Semi-Arid Regions, vol. 21. Water Science and Technology Library, Kluwer Academic Publishers, Norwel, Massachusetts.
9. Ben-Sasson, M., Brenner, S., Paldor, N., 2009. Estimating air-sea heat fluxes in semi-enclosed basins: the case of the Gulf of Eilat (Aqaba). *Journal of Physical Oceanography*, **39**: 185–202.
10. Chapuis, R.P. 2004. Predicting the saturated hydraulic conductivity of sand and gravel using effective diameter and void ratio. Canadian Geotechnical Journal, **41**, 787–795.
11. Chongxun, M., Fanggui, L., Mei, Y., Rongyong, M., Guikai, S. 2008. Risk analysis for earth dam overtopping, *Water Science and Engineering*, **1**, 76- 87.
12. Cools, J., Vanderkimpen, P., El Afandi, G., Abdelkhalek, A., Fockedey, S., El Sammany, M., Abdallah, G., El Bihery, M., Bauwens, W., Huygens, M. 2012. An early warning system for flash floods in hyper-arid Egypt. *Natural Hazards and Earth System Science*, **12**, 443–457.
13. Cullen, H.M., Kaplan, A., Arkain, P.A., Damenocal, P.B., 2002. Impact of North Atlantic Oscillation on Middle Eastern climate and streamflow. *Climatic Change*, **55**, 315-338.
14. Dayan, U., Ziv, B., Margalit, A., Morin, E., Sharon, D., 2001. A severe autumn storm over the Middle-East: synoptic and mesoscale convection analysis*. Theoretical & Applied Climatology*, **69**, 103-122.
15. Eliwa, H.A., Kimura, J-I., T. Itaya, T., 2006. Late Neoproterozoic Dokhan Volcanics, North Eastern Desert, Egypt: Geochemistry and petrogenesis. *Precambrian Research,* **151**: 31–52.

16. El-Magd, I.A., Hermas, E.S., Bastawesy, M.E., 2010. GIS-modelling of the spatial variability of flash flood hazard in Abu Dabbab catchment, Red Sea Region, Egypt. The Egyptian *Journal of Remote Sensing and Space Sciences*, **13**: 81-88.
17. El-Shamy, I.Z., 1992. Recent recharge and flash flooding opportunities in the Eastern Desert. *Annuals of the Geological Survey of Egypt*, **8**: 323-334.
18. El-Sawy, E.K., Bekheit, M.H., Abd El-Motaal, E., Orabi A. A., Abd El Gany, M.K., 2011. Geo-environmental studies on Wadi Qena, Eastern Desert, Egypt, by using remote sensing data and GIS. *Al-Azhar Bulletin of Science,* **22**: 33-60.
19. Elsadek, W.M., Ibrahim, M.G., Mahmod, W.E. 2018. Flash flood risk estimation of Wadi Qena watershed, Egypt using GIS based morphometric analysis. *Applied Environmental Research*, **40**, 36-45.
20. Eshel, G., Farrell, B.F., 200. Mechanisms of eastern Mediterranean rainfall variability. *Journal of Atmospheric Sciences,* **57**, 3219-3232.
21. Farhan, Y. and Anaba, O., 2016. Flash flood risk estimation of Wadi Yutum (Southern Jordan) watershed using GIS based morphometric analysis and remote sensing techniques. *Open Journal of Modern Hydrology*, **6**: 79-100.
22. Fick, S.E. and R.J. Hijmans, R.J., 2017. WorldClim2: new 1-km spatial resolution climate surfaces for global land areas. *International Journal of Climatology*, DOI: 10.1002/joc.5086.
23. Gabr, S. and El Bastawesy, M., 2015. Estimating the flash flood quantitative parameters affecting the oil-fields infrastructures in Ras Sudr, Sinai, Egypt, during the January 2010 event. *The Egyptian Journal of Remote Sensing and Space Sciences*, **18**: 137-149.
24. Geith, H. and Sultan, M., 2002. Construction of a hydrological model for estimating wadi runoff and groundwater recharge in the Eastern Desert, Egypt. *Journal of Hydrology*, **263**: 36-55.
25. Grant, G.E., 1997. Critical flow constrains flow hydraulics in mobile bed streams: a new hypothesis. *Water Resources Research*, **33**, 349–358.
26. Greenbaum, N., 2002. Paleofloods and the estimation of long term transmission losses and recharge to the lower Nahal Zin alluvial aquifer, Negev desert, Israel. Pp. 311- 328 In: Ancient Floods, Modern Hazards: Principles and Applications of Paleoflood Hydrology, Water Science and application Vol. **5,** House, P.K., Webb, R.H., Baker, V.R., Levish, D.R. (Editors), ABU Publication,Washington.
27. Greenbaum, N., Schwartz, U., Carling, P.A., Bergman, N., Mushkin, A., Zituni, R., Halev, R., Benito, G., Porat, N., 2020. Frequency of boulders transport during large floods in hyperarid areas using paleoflood analysis – An example from the Negev Desert, Israel. *Earth-Science Reviews*, **202**: 103086
28. Hobbs, J.J. 1990. *Bedouin Life in the Egyptian Wilderness*. The American University in Cairo Press, Cairo, 165pp.
29. Hydrologic Engineering Center, 1998. Flood Hydrograph Package User’s Manual June 1998. Hydrologic Engineering Center, US Army Corps of Engineers, Davis, CA, 434pp.
30. Ismail, I., Othman, A., Abd El-Latif, R. and Ahmed, A., 2010. Impact of flash flood on development potentials of Wadi Abu Ghusun, Eastern Desert, Egypt. *Kuwait Journal of Science and Engineering*, **37**: 111-134.
31. Kassa, M. and Girgis, W.A., 1964. Studies of the ecology of the Eastern Desert, Egypt, I. The region between lat. 27^{o} 30’ N and Lat. 25^{o} 30’ N. *Bulletin de la Société de Géographie d’Égypte*, **41-42**: 43-72.
32. Katz, T., Ginat, H., Eyal, G., Steiner, Z., Braun, Y., Shalev, S., Goodman-Tchernov, B.N., 2015. Desert flash floods form hyperpycnal flows in the coral-rich Gulf of Aqaba, Red Sea. *Earth and Planetary Science Letters*, **417**: 87-98.

33. Kehew, A.E., Milewski, A., Soliman, F., 2010. Reconstructing an extreme flood from boulder transport and rainfall–runoff modelling: Wadi Isla, South Sinai, Egypt. *Global and Planetary Change*, **70**: 64–75.
34. Labib, T.M., 1981. Soil erosion and total denudation due to flash floods in the Egyptian eastern desert. *Journal of Arid Environments,* **4**: 191-202.
35. Makovicky, E., Frei, R., Karup-Møller, S., Bailey, J.C., 2016. Imperial Porphyry from Jebel Abu Dokhan, the Red Sea Mountains, Egypt Part I. Mineralogy, petrology and occurrence. *Neues Jahrbuch für Mineralogie*, 193: 1–27.
36. Moawad B.M., 2012. Predicting and analyzing flash floods of ungauged small-scale drainage basins in the Eastern Desert of Egypt. *Journal of Geomatics,***6**, 23–30.
37. Moawad, B.M., 2013. Analysis of the flash flood occurred on 18 January 2010 in wadi El Arish, Egypt (a case study), *Geomatics, Natural Hazards and Risk*, **4**, 254-274.
38. Moawad, B.M., Abdel Aziz, A.O., Mamtimin, B., 2016. Flash floods in the Sahara: a case study for the 28 January 2013 flood in Qena, Egypt, *Geomatics, Natural Hazards and Risk*, **7**:215-236.
39. Moeyersons, J., Vermeersch, P.M., Beeckman, H., Van Peer, P., 1999. Holocene environmental changes in the Jebel Umm Hammad, Eastern Desert, Egypt. *Geomorphology*, **26**: 297–312.
40. Mohamed, S.A. 2019. Application of satellite image processing and GIS-Spatial modeling for mapping urban areas prone to flash floods in Qena governorate, Egypt. *Journal of African Earth Sciences*, **158**, 103507.
41. Moneim, A.A.A., 2005. Overview of the geomorphological and hydrogeological characteristics of the Eastern Desert of Egypt. *Hydrogeology Journal*, **13**: 416–425.
42. Nicholson, S., 1997. Nicholson's Africa precipitation. National Center for Atmospheric Research. http://dss.ucar.edu/catalogs/atmlists/precip.html
43. Reid, I., Laronne, J.B., Powell, D.M., 1995**.** The Nahal Yatir bedload database: ephemeral stream sediment dynamics in a gravel-bed. *Earth Surface Processes and Landforms***, 20**,845-857.
44. Said, R., 1990. The Geology of Egypt, Ed., Balkema, Rotterdam, pp. 9-25.
45. Shentsis, I., Meirovich, L., Ben-Zvi, A., Eliyahu Rosenthal, E., 1999. Assessment of transmission losses and groundwater recharge from runoff events in a wadi under shortage of data on lateral inflow, Negev, Israel. *Hydrological Processes*, **13**, 1649-1663.
46. Schwartz, U., Schick, A. P. 1990. Water in an alluvial fill in a hyper-arid region. *Horizons in Geography*, **31**, 109-122.
47. Stephens, T. 2010. Manual on small earth dams: A guide to siting, design and construction. FAO Irrigation and Drainage Paper 64, 114pp, Food and Agriculture Organization of the United Nations, Rome.
48. Sumi, T., Saber, M., Kantoush, S.A., 2013. Japan-Egypt hydro network: science and technology collaborative research for flash flood management. *Journal of Disaster Research*, **8**: 28-36.
49. Tregenza, L.A., 1955. *The Red Sea Mountains of Egypt*. Oxford University Press, London.
50. Wilkinson, J., 1832. Notes on a part of the Eastern Desert of Upper Egypt. *The Journal of the Royal Geographical Society of London*, **2**: 28-60.
51. Yair, A., Danin, A. 1980. Spatial variations in vegetation as related to the soil moisture regime over an arid limestone hillside, northern Negev, Israel. *Oecologia*, **47**, 83-88.
52. Yehia, M.A., Ashmawy, M.H., El Etr, H.A., Abdel Monsef, H., El Shamy, I.Z., Hermas, E.A., Higazy, M.N., Hassan, S.M., 1999. Flash flooding threat to the Red Sea coastal towns of Safaga, Quseir and Marsa El Alam. *Egyptian Journal of Remote Sensing and Space Science*, **2**: 69-86.
53. Zaid, S.M., 2009. Potential of flash flooding of the drainage bain of Quseir area and risk evaluation. Fourth Environmental Conference, Faculty of Science, Zagazig University, 1-16.